4-27-2003

Be-10/Be-7 tracer of atmospheric transport and stratosphere-troposphere exchange

C. Jordan
University of New Hampshire

Jack E. Dibb
University of New Hampshire, jack.dibb@unh.edu

R C. Finkel
Lawrence Livermore National Laboratory

Recommended Citation
Jordan, C. E., J. E. Dibb, and R. C. Finkel (2003), 10Be/7Be tracer of atmospheric transport and stratosphere-troposphere exchange, J. Geophys. Res., 108, 4234, doi:10.1029/2002JD002395, D8.

$^{10}Be/^{7}Be$ tracer of atmospheric transport and stratosphere-troposphere exchange

C. E. Jordan
National Research Council, NASA Langley Research Center, Hampton, Virginia, USA

J. E. Dibb
Climate Change Research Center, University of New Hampshire, Durham, New Hampshire, USA

R. C. Finkel
Center for Accelerator Mass Spectrometry, Lawrence Livermore National Laboratory, Livermore, California, USA

Received 28 March 2002; revised 22 August 2002; accepted 5 December 2002; published 17 April 2003.

[1] The $^{10}Be/^{7}Be$ ratio is a sensitive tracer of atmospheric transport and stratosphere-troposphere exchange (STE). Data from five NASA aircraft field missions (PEM: West A and B, Tropics A; SONEX; and SUCCESS) have been assembled to produce the largest data set of ^{10}Be, ^{7}Be, and their ratio collected to date (>300 samples). Ratios near 0.60 are indicative of tropospheric air with little stratospheric influence, while higher ratios are found in stratospheric air. Samples from the lower stratosphere were all collected within 2.5 km of the tropopause and had ratios >1.27. Of these lower stratosphere samples only 16% had ratios in excess of 3.0, suggesting that higher ratio air resides away from the tropopause. Seasonality observed in the $^{10}Be/^{7}Be$ ratios results from the downwelling of air with elevated ratios from higher in the stratosphere in the spring and summer (midlatitudes) and from the decay of ^{7}Be during descent in the winter polar vortex (high latitudes). Our results illustrate the complexity of STE and some of the mechanisms through which it occurs, including tropopause folding, mixing associated with subtropical jets, and the effect of synoptic systems such as hurricanes and northeasters. The $^{10}Be/^{7}Be$ ratio provides important information beyond that which can be derived from studies that rely on chemical mixing ratios alone. *INDEX TERMS:* 0305 Atmospheric Composition and Structure: Aerosols and particles (0345, 4801); 0368 Atmospheric Composition and Structure: Troposphere—constituent transport and chemistry; 3362 Meteorology and Atmospheric Dynamics: Stratosphere/troposphere interactions; *KEYWORDS:* Aerosols, radioisotopes, beryllium, stratosphere-troposphere exchange

Citation: Jordan, C. E., J. E. Dibb, and R. C. Finkel, $^{10}Be/^{7}Be$ tracer of atmospheric transport and stratosphere-troposphere exchange, *J. Geophys. Res.*, *108*(D8), 4234, doi:10.1029/2002JD002395, 2003.

1. Introduction

[2] Stratosphere-troposphere exchange is a complex process that appears to be neither geographically nor seasonally uniform. For example, *Folkins et al.* [1999] have recently suggested that in the tropics air from the marine boundary layer at Samoa (14°S) is only convected to a height of 14 km, 3 km short of the tropopause height. They observed a clearly defined O_3 chemopause at this low altitude and they proposed that above this altitude, in the upper troposphere, O_3 is produced in situ and then ascends slowly into the stratosphere. This observation is in contrast to that of others who have suggested that elevated O_3 below the tropopause is due to stratospheric air that has mixed down into the troposphere [e.g., *Tuck et al.*, 1997; *Fujiwara et al.*, 1998].

[3] Another mechansim for STE is via tropopause folds in midlatitudes [*Danielsen*, 1968; *Danielsen and Hipskind*, 1980; *Kritz et al.*, 1991]. Such folds occur near the jet stream [*Danielsen*, 1968; *Danielsen et al.*, 1987] when a layer of air is extruded from the lower stratosphere on the cyclonic (poleward) side of the jet. This stratospheric air enters the troposphere beneath the core of the jet and moves equatorward and downward toward the surface boundary layer [*Danielsen et al.*, 1987]. Tropopause folds can also bring tropospheric air into the stratosphere, making the lower stratosphere a transition layer between the troposphere and the stratospheric overworld [*Danielsen*, 1968].

[4] Seasonality in the source of stratospheric air entering the troposphere can occur even though the actual intensity of STE does not vary. The influence of the subtropical jet is minimal on the lowermost stratosphere, hence actual STE is fairly consistent year-round [*Dethof et al.*, 2000]. However, as the jet strengthens in winter, exchange between the stratospheric overworld and lower stratosphere is suppressed [*Dethof et al.*, 1999, 2000]. As a result the stratospheric air entering the troposphere in winter includes less overworld air than stratospheric air entering in spring and summer when

0148-0227/03/2002JD002395

the weakened jet allows more overworld air to descend. Measurements made in September at 34.5°N show most of the air in the lowermost stratosphere had been transported quasi-isentropically from the troposphere [*Ray et al.*, 1999], while observations in May and June (at 34.5°N and 64.5°N, respectively) showed the air had been predominantly advected down from the overworld [*Ray et al.*, 1999].

[5] Synoptic systems may also affect STE. *Dethof et al.* [2000] suggest that mixing may be enhanced at the end of the Atlantic storm track in winter and downstream of the Asian monsoon anticyclone in summer. Enhanced $^{33}P/^{32}P$ ratios reported by *Benitez-Nelson and Buesseler* [1999] were attributed to synoptic systems such as hurricanes and northeasters drawing down stratospheric air (signified by high ratios) into the troposphere. Although, beryllium bound to aerosols tends to be washed out of the troposphere by precipitation, *Aldahan et al.* [2001] found peaks in ^{7}Be concentrations at the end of heavy precipitation events. They attributed this to stratospheric influx.

[6] The complexity of the mixing processes associated with STE and the seasonality of the effects have made the process difficult to characterize fully. ^{10}Be, ^{7}Be, and the ^{10}Be/^{7}Be ratio are important tracers that can be used to provide new information about STE. ^{10}Be and ^{7}Be are produced by cosmic ray interactions with atmospheric oxygen and nitrogen. In 1981, *Raisbeck et al.* suggested that the ratio of the cosmogenic radioactive isotopes of beryllium, ^{10}Be/^{7}Be, could be used as a probe of atmospheric transport. Since then only a handful of studies have reported ^{10}Be in either aerosols [*Raisbeck et al.*, 1981; *Dibb et al.*, 1994] or precipitation [*Monaghan et al.*, 1986; *Brown et al.*, 1989]. In this paper, we present the largest data set of ^{10}Be, ^{7}Be, and their ratio collected to date. Both isotopes are produced by cosmic ray spallation, predominantly in the midlatitude stratosphere, and then are rapidly taken up by aerosols. Aerosols can remain aloft in the stratosphere for years. Because of the vastly different half-lives of ^{10}Be and ^{7}Be, 1.5×10^{6} years and 53 days, respectively, the ratio of these species will increase in the stratosphere as the aerosols age.

[7] Eventually, stratospheric aerosols are transported into the troposphere where they are removed from the atmosphere via scavenging and deposition. The residence time of aerosols in the troposphere is about 30–40 days [*Shapiro and Forbes-Resha*, 1976], which is insufficient to allow the ^{10}Be/^{7}Be ratio to increase appreciably above its production ratio. Since there is no evidence for isotopic fractionation during either aerosol uptake or tropospheric removal processes, the ratio will retain its stratospheric signature even if mixing ratios change significantly.

[8] In an isolated air mass where the only loss is due to radioactive decay, ^{10}Be will accumulate with negligible decay, while ^{7}Be will approach secular equilibrium where decay balances production. Secular equilibrium for ^{7}Be will be reached in approximately 8 months. Once ^{7}Be has reached secular equilibrium, the ^{10}Be/^{7}Be ratio will increase at a rate that depends only on the ^{10}Be production rate. Assuming ^{10}Be is produced at 60% the rate of ^{7}Be [*Dibb et al.*, 1994; *Nagai et al.*, 2000], the ratio will increase over time from its initial value of about 0.6 to a ratio of 5.8 after 2 years and to 11.6 after 4 years. In the stratosphere, three factors affect the observed ratio. First, if an air parcel moves from a region of high production to a region of lower production the ^{10}Be/^{7}Be ratio will increase as ^{7}Be decays to the new, lower secular equilibrium value. Second, if air mixes between regions of differing age (e.g., the stratosphere and troposphere) the resulting air mass will have an intermediate ratio that reflects the relative influence of the respective source regions. Third, gravitational settling of aerosols-bound beryllium results in mid and upper stratosphere ratios that are lower than would be expected from the air parcel residence time alone, because removal from the source region keeps the ratio nearer the production ratio. These attributes make the beryllium ratio a useful tracer for stratosphere-troposphere exchange (STE).

[9] Note that there is a fourth factor to be considered. Although, for the purposes of the discussion here, the production ratio of ^{10}Be/^{7}Be is assumed to be constant at 0.60, it may in fact vary somewhat between the stratosphere and troposphere, and also as a function of latitude. *Nagai et al.* [2000] calculated the production rates of ^{10}Be and ^{7}Be and found the global average production rate in the stratosphere of 0.44 during solar minimum, while in the troposphere they found 0.67. They suggest multiplying these by 0.8–0.9 to better estimate long-term averages, which results in a production rate of 0.35–0.40 in the stratosphere, and 0.53–0.60 in the troposphere. Here, we will use the higher tropospheric value as a typical production ratio. This is a conservative mean value to distinguish observations of higher stratospheric ratios from lower tropospheric ones. Further, *Nagai et al.* [2000] calculations indicated an increase in the production ratio with latitude, for the stratosphere, this increase was observed above 80°, but in the troposphere, the increase was seen above 50°. Nonetheless, even at high latitudes, the production ratio does not exceed 1.0. Hence, ratios above this value always reflect increasing age in an air mass as ^{10}Be accumulates while ^{7}Be maintains its secular equilibrium.

[10] A recent modeling experiment has shown the region of the stratosphere with the highest ^{10}Be/^{7}Be ratios lies between 20 and 40 km in the tropical stratosphere, with the peak ratios exceeding 8.0 between 25 and 30 km [*Bergmann et al.*, 2001]. Nearer the tropopause, the ratios are lower, approximately 2.0. The seasonal behavior described above suggests that the ^{10}Be/^{7}Be ratio should increase in the lower stratosphere in the spring and summer under the influence of descending stratospheric overworld air with higher ^{10}Be/^{7}Be ratios. In the fall and winter, as the influence of this source wanes, it is expected the ratio will decrease as tropospheric influx becomes dominant.

[11] Using the ratio of ^{10}Be/^{7}Be, *Dibb et al.* [1994] found that stratospheric influence on the Arctic troposphere was nearly continuous year-round. More importantly, they showed that the ratio peaked in late summer, indicating that the greatest stratospheric influence occurred at that time even though the mixing ratios of the two isotopes independently were at their minima. The mixing ratios alone would suggest a tropospheric air mass with little or no stratospheric input. Yet the isotope ratio clearly revealed a stratospheric signature unaffected by the processes that removed the beryllium bearing aerosols from the Arctic troposphere.

[12] We present here an overview of an extensive data set of ^{10}Be/^{7}Be ratios in the context of other chemical constituents and discuss the results in terms of STE. Three case studies illustrate how the ^{10}Be/^{7}Be ratio may lead to a better understanding of the complexities of stratosphere-tropo-

sphere exchange dynamics sketched out in the preceding discussion.

2. Methods

2.1. Sampling and Sample Selection

[13] We have measured the concentrations of ^{7}Be and ^{210}Pb in aerosols collected from the NASA DC-8 on a series of NASA campaigns as part of the Global Tropospheric Experiment (GTE) and of the Atmospheric Effects of Aviation Project Subsonic Assessment (AEAP SASS). The specific campaigns discussed here are GTE's Pacific Exploratory Missions (PEM) West (A and B) and Tropics A, SASS Subsonic Aircraft: Cloud and Contrail Effects Special Study (SUCCESS), and the Ozone and Nitrogen Oxide Experiment (SONEX). *Dibb et al.* [1996, 1997, 1998, 1999, 2000] have discussed the ^{7}Be and ^{210}Pb results from these campaigns and have described the airborne aerosol sampling system and protocols that were used.

[14] An earlier investigation of ^{10}Be/^{7}Be as an atmospheric tracer in the high Arctic relied on ^{10}Be measurements in 8 samples collected during PEM West A and 6 collected during AGASP 3 [*Dibb et al.*, 1994]. These results are incorporated into the present analysis, but are dwarfed in number by new measurements of ^{10}Be during the PEM West B (32 samples), SUCCESS (58 samples), SONEX (143 samples), and PEM Tropics A (66 samples) campaigns. Targets for ^{10}Be analysis were only prepared from samples that contained more than 5×10^5 atoms of ^{7}Be. Although this selection criteria was necessary to ensure that there would be sufficient ^{10}Be to quantify with good accuracy, it does bias our data set to include more upper tropospheric samples with significant stratospheric influence than would be representative of the study regions. The mean standard deviations for ^{7}Be, ^{10}Be, and the ratio, ^{10}Be/^{7}Be are 12%, 9%, and 14%, respectively.

2.2. Target Preparation and Accelerator Mass Spectrometry

[15] ^{210}Pb had previously been determined by alpha spectrometry for all of the samples discussed here, as described by *Dibb et al.* [1996]. The acid leach generated in this process, and the leached filter, had been retained. In the present study these filters were pulverized and leached again in 6 N HCl. This slurry was filtered and the liquid combined with the archived acid leach. Beryllium was then separated using cation exchange chromatography, $Be(OH)_2$ precipitated with NH_4OH and BeO prepared by igniting the purified precipitate. Targets were initially prepared by mixing pure Ag powder with the BeO (all samples from PEM West A, B and SUCCESS). Later targets were mixed with Nb instead of Ag to enhance BeO-currents in the Cs sputter source of the Lawrence Livermore National Laboratory (LLNL) FN accelerator mass spectrometer. This change in procedure was made for samples from SONEX and PEM Tropics A. Targets were sent to LLNL for analysis in the Center for Accelerator Mass Spectrometry AMS system, *Davis et al.* [1990]. ^{10}Be concentrations were normalized to an ICN ^{10}Be standard prepared by K. Nishiizumi.

3. Results

[16] Selected aerosol samples collected during five different NASA field campaigns (PEM West A and B, PEM Tropics A, SONEX, and SUCCESS) were analyzed. In addition to both ^{7}Be and ^{10}Be, ancillary data from these campaigns include O_3 (all missions); CO_2, CH_4, and CO (all but PEM West A); HNO_3 (PEM West B, PEM Tropics A, and SONEX); and N_2O (PEM West B, SONEX, and SUCCESS). In addition, on three missions (PEM Tropics A, SONEX, and SUCCESS) the height of the tropopause was determined from microwave temperature profile (MTP) data. Overall, the data set includes 300 samples for which the ratio of ^{10}Be to ^{7}Be has been determined.

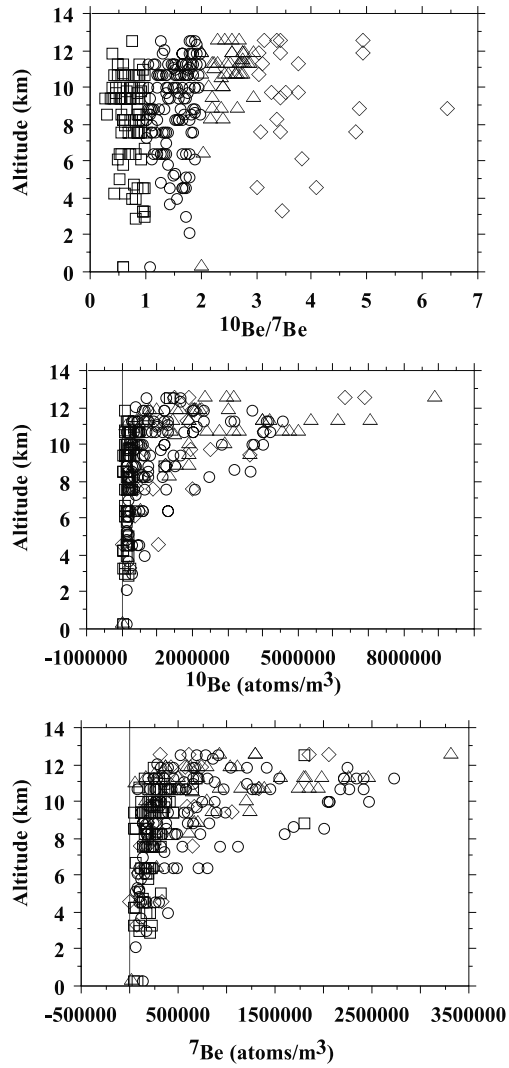

Figure 1. ^{10}Be/^{7}Be, ^{10}Be, and ^{7}Be plotted versus altitude, grouped according to the value of the ^{10}Be/^{7}Be ratio: <1.0 (group 1, squares), 1.0–2.0 (group 2, circles), 2.0–3.0 (group 3, triangles), and >3.0 (group 4, diamonds).

[17] In general, both ^{10}Be and ^{7}Be increase with altitude (Figure 1). Although low mixing ratios for ^{10}Be and ^{7}Be ($<2.0 \times 10^6$ atoms/m^3 and $<0.5 \times 10^6$ atoms/m^3, respectively) are sometimes observed at even the highest altitudes, the maximum value observed tends to increase with height as does the number of samples that show high ratios. Below 4 km, the mixing ratios for both radioisotopes do not exceed these thresholds, reflecting the loss mechanisms that remove the beryllium bearing aerosols from the troposphere.

Table 1. Summary of Be Isotopes and Selected Gas Phase Tracer Measurements

			^{10}Be/^{7}Be	^{7}Be, atoms/m^3 $\times 10^3$	^{10}Be, atoms/m^3 $\times 10^3$	O_3, ppbv	HNO_3, pptv	CO_2, ppmv	N_2O, ppbv	CH_4, ppbv	CO, ppbv
Distance from TP											
<0 km	Strat	Mean	2.42	1230	2990	250	609	362	304	1700	64
		Min-Max	1.27–4.91	360–3310	660–8860	79–652	146–1099	358–367	278–313	1595–1764	14–153
		# of Samples	32	32	32	28	10	28	24	28	28
>0 km	Trop	Mean	1.62	550	960	104	248	362	310	1737	82
		Min-Max	0.27–6.46	80–2720	80–4170	29–387	10–1037	359–370	303–314	1687–1789	31–189
		# of Samples	91	91	91	89	57	88	51	85	89
^{10}Be/^{7}Be											
$1.0 \leq x < 2.0$	Strat 2	Mean	1.72	1130	1950	174	570	362	309	1720	62
		Min-Max	1.27–1.99	450–2400	660–4550	79–267	146–1099	360–365	304–312	1688–1752	28–110
		# of Samples	13	13	13	13	8	13	11	13	13
$2.0 \leq x < 3.0$	Strat 3	Mean	2.65	1380	3700	313		362	301	1690	70
		Min-Max	2.02–2.94	360–3310	770–8860	106–621		358–367	280–313	1604–1764	14–153
		# of Samples	14	14	14	10	0	10	10	10	10
>3.0	Strat 4	Mean	3.58	1090	3710	323	763	361	296	1669	55
		Min-Max	3.04–4.91	420–2050	1910–6920	184–652	674–851	358–364	278–306	1595–1722	15–110
		# of Samples	5	5	5	5	2	5	3	5	5
<1.0	Trop 1	Mean	0.67	280	190	53	122	361	313	1739	79
		Min-Max	.27–.99	140–500	80–490	29–100	10–281	359–365	313–314	1697–1789	52–116
		# of Samples	29	29	29	28	24	28	6	28	28
$1.0 \leq x < 2.0$	Trop 2	Mean	1.46	740	1140	110	345	362	311	1740	81
		Min-Max	1.01–1.97	80–2720	110–4160	43–387	11–1037	359–370	306–314	1693–1783	31–189
		# of Samples	39	39	39	38	29	37	26	35	38
$2.0 \leq x < 3.0$	Trop 3	Mean	2.50	660	1620	152	376	363	309	1725	84
		Min-Max	2.14–2.78	160–1810	340–4170	35–293	44–782	360–366	303–313	1687–1764	33–116
		# of Samples	13	13	13	13	3	13	10	12	13
>3.0	Trop 4	Mean	3.82	460	1640	163	75	364	308	1736	90
		Min-Max	3.03–6.46	190–740	660–2520	59–248	75	361–367	306–313	1704–1769	64–118
		# of Samples	10	10	10	10	1	10	9	10	10
Mission											
All Data		Mean	1.82	730	1490	139	302	362	308	1728	78
		Min-Max	.27–6.46	80–3310	80–8860	29–652	10–1099	358–370	278–314	1595–1789	14–189
		# of Samples	123	123	123	117	67	116	75	113	117
PEM Tropics A		Mean	1.13	350	560	72	155	361		1710	63
		Min-Max	.27–3.44	110–1330	80–4040	29–278	10–851	359–361		1660–1778	30–94
		# of Samples	29	29	29	27	26	26	0	25	27
SONEX		Mean	1.45	910	1420	118	395	362	310	1744	70
		Min-Max	.45–6.46	140–2720	160–4550	35–387	35–1099	361–363	304–314	1690–1789	28–113
		# of Samples	44	44	44	44	41	44	29	42	44
SUCCESS		Mean	2.56	790	2080	199		364	307	1723	93
		Min-Max	.89–4.91	80–3310	110–8860	46–652		358–370	278–314	1595–1776	14–189
		# of Samples	50	50	50	46	0	46	46	46	46

[18] The ^{10}Be/^{7}Be ratio exhibits a different behavior (Figure 1). Relatively high ratios are seen down to 4 km and even below. Further, high ratios are observed throughout the observed altitude range, even when the mixing ratios are low (Figure 1). It is difficult to interpret the ^{10}Be/^{7}Be ratio as a function of altitude alone. However, if tropopause height is used to separate the samples collected in the stratosphere from those obtained in the troposphere, a clearer picture emerges of the distribution of this ratio in the atmosphere.

[19] Tropopause height (determined by remotely sensed temperature measurements) is available for a subset (123 samples) of the overall data set (300 samples). The mean, minimum, and maximum values for a number of parameters are given for this subset in Table 1, along with the number of samples collected either above or below the tropopause. None of the stratospheric samples were collected more than 2.5 km above the tropopause. Hence, these samples reflect only the lowermost stratosphere. Also, only ^{7}Be samples above the 5×10^5 atom threshold were analyzed for ^{10}Be. Since the presence of elevated ^{7}Be often indicates the presence of stratospheric air in the sample, there may be a slight bias in the tropospheric data (Table 1). As expected, both beryllium radioisotopes, O_3, and HNO_3, all have higher mean mixing ratios in the stratosphere than in the troposphere, while CH_4, CO, and N_2O tend to be higher in the troposphere. CO_2 is fairly uniformly mixed.

[20] To evaluate the relation between the ^{10}Be to ^{7}Be ratio and stratosphere-troposphere exchange, we further subdivided the stratospheric and tropospheric samples into four subgroups according to the value of the ratio: group one ratios are less than 1.0, group two ranges from 1.0 to 2.0, group three ranges from 2.0 to 3.0, and group 4 ratios are equal to or exceed 3.0. The means, minima, and maxima for these subgroups are also given in Table 1. The results of this grouping are illustrated graphically in Figure 2 as a function of distance from the tropopause, with the data partitioned into stratospheric and tropospheric samples (Figure 2, upper panel). The middle panel shows the same data, but split into

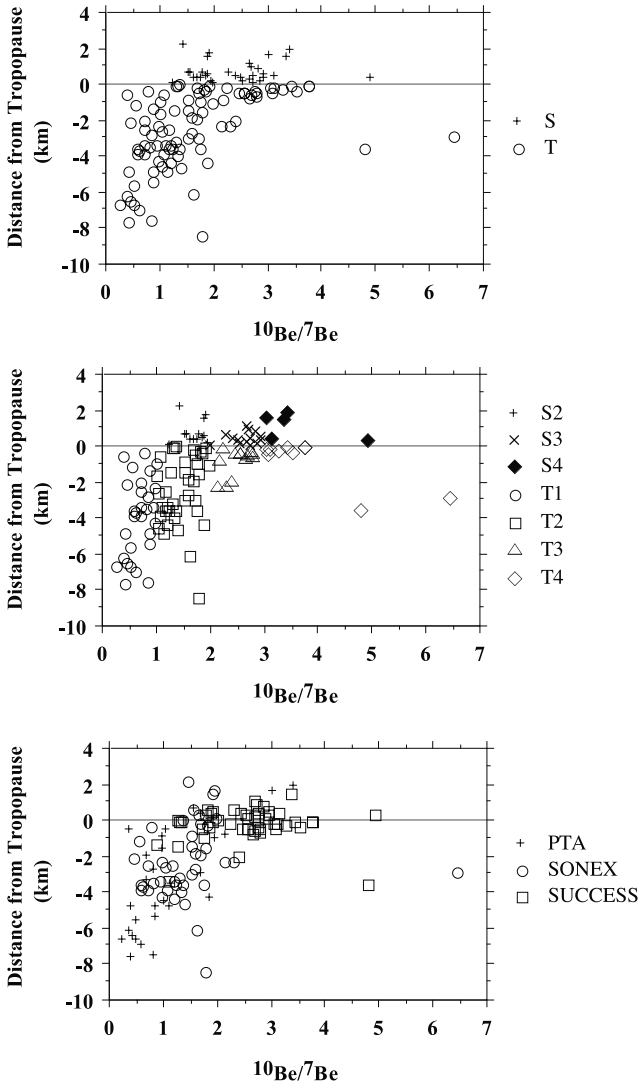

Figure 2. ^{10}Be/^{7}Be plotted versus distance from the tropopause. Top panel shows the difference between stratospheric and tropospheric samples. Middle panel further subdivides these according to the value of the ^{10}Be/^{7}Be ratio, the groups defined as in Figure 1 caption. Bottom panel shows the ratios observed on three different field missions.

the four subgroups. Since none of the stratospheric samples have a ratio <1.27, there is no group S1.

[21] This absence of low ratios in the stratosphere suggests that values near the 0.60 production ratio mostly or entirely result from tropospheric production. As expected, the mixing ratios of both ^{10}Be and ^{7}Be are correspondingly low for the tropospheric group 1 samples (T1; Table 1). Group T1 has the lowest mean and maximum mixing ratios for both beryllium isotopes. This is also true for O_3, and is generally true for HNO_3, except for T4 (only one sample in this group had a HNO_3 measurement).

[22] The ^{10}Be/^{7}Be ratio tends to be higher in the stratosphere than the troposphere (Figure 2; Table 1), however some of the highest values of the ^{10}Be:^{7}Be ratio were found in samples collected in the troposphere. These high ratio tropospheric samples must be indicative of stratospheric air entering the troposphere, because tropospheric air cannot age sufficiently for such high ratios to develop. Only 16% of the stratospheric samples belong to the highest ratio group, suggesting that stratospheric air near the tropopause generally has a low characteristic ratio. Most of the high ratio samples in both the stratosphere and troposphere were collected during the SUCCESS field campaign, which was conducted over the central United States in April and May of 1996 (Figure 2, bottom panel). The other two field campaigns for which we have the tropopause height were carried out during northern hemisphere autumn: September–November in 1996 (PEM-Tropics A) and 1997 (SONEX). Transport scenarios reported by *Dethof et al.* [2000] suggest that the weakening of the subtropical jets in spring and summer allows the flux of stratospheric overworld air downward into the lower stratosphere. From there, it can be exchanged isentropically with the troposphere. If this scenario is true, we would expect tropospheric samples with high ratios to be centered near the tropopause break. The SUCCESS samples (Figure 3) do cluster around 40° N. Thus this data supports a scenario in which older overlying stratospheric air descends in spring and enters the troposphere from the lower stratosphere. This scenario agrees with prior results indicating a greater influence of stratospheric overworld air in the lower stratosphere in the spring [*Ray et al.*, 1999].

[23] A closer examination of ^{10}Be/^{7}Be ratio as a function of latitude and longitude (Figure 3) reveals that most stratospheric air was found around 40° (median absolute latitude, the mean, 44° reflects five high latitude samples above 60°). The oldest air in both the stratosphere and troposphere, based on the ^{10}Be/^{7}Be ratio, was found at a median latitude of 40° (means of 43° and 40°, respectively). S4 air was observed at latitudes ranging from 37° to 57°, while T4 air was encountered at latitudes ranging from 36° to 48°. Clearly, there are processes leading to the influx of stratospheric air originating well above the tropopause into the troposphere at these midlatitudes.

[24] The stratospheric samples collected closest to the poles (between 60° and 71°) lie in group S2, typical of air that resides near the tropopause throughout the stratosphere. However, high ratio samples, typical of groups S3 or S4, have been observed near the high-latitude tropopause [*Dibb et al.*, 1994; *Raisbeck et al.*, 1981], perhaps originating from the loss of ^{7}Be as higher altitude air descends from a region of greater ^{7}Be and ^{10}Be production to a region with lower production [*Raisbeck et al.*, 1981; *Dibb et al.*, 1994]. The recent modeling study by *Bergmann et al.* [2001] corroborates this scenario. Their results predict a layer of enhanced ratio just above the tropopause peaking just above 3.0 and then decreasing with increasing altitude [*Bergmann et al.*, 2001]. While the peak in ratios observed by *Dibb et al.* [1994] is somewhat higher (ranging from 4.0 to 6.9), slow descent is able to explain such high near-tropopause ratios in this region. Assuming a descent rate of 0.08 cm/s for the Arctic at an altitude of 19 km [*Schoeberl et al.*, 1992], it would take 144 days for an air parcel to descend to 9 km. *Dibb et al.* [1994] report a ratio of 2.4 observed at 19 km in the Arctic and higher ratios, 4.0–6.9 near the tropopause. Given the ^{7}Be half-life of 53 days, this is sufficient time for ^{7}Be decay to increase the ^{10}Be/^{7}Be ratio to these values. All of the high value

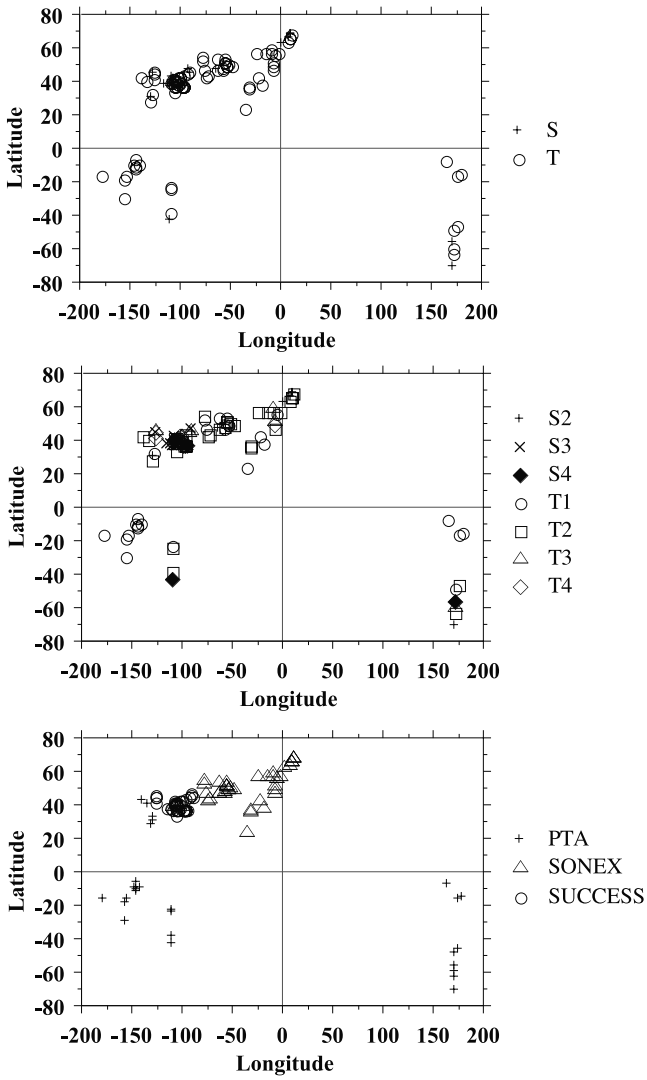

Figure 3. The locations where the samples were collected. Top panel shows the difference between stratospheric and tropospheric samples. Middle panel further subdivides these according to the value of the ^{10}Be/^{7}Be ratio, the groups defined as in Figure 1 caption. Bottom panel divides the data according to the field mission during which the sample was obtained.

ratios at high latitudes were observed in spring and summer. Observations in the tropopause region during the fall ranged from 0.6–2.2. This suggests the descent is associated with the polar vortex in winter.

[25] The ^{10}Be/^{7}Be ratio yields more information than either ^{7}Be or ^{10}Be alone. All of the ^{7}Be T1 mixing ratios are below 0.5×10^{6} atoms/m^{3} (Figure 4, Table 1), which reflects the predominantly tropospheric origin of these samples. Similarly, the ^{10}Be T1 mixing ratios (Figure 5) are all uniformly low, which corroborates the suggestion that T1 data is due to in situ production in the troposphere. Aerosols here are scavenged too quickly to allow for the buildup of ^{10}Be with age. The mixing ratios for both isotopes in the T4 group, however, are not at the high end of the observed range. Mixing and removal processes have reduced the amount of beryllium in the troposphere in such a way that using the mixing ratios alone would not indicate the presence of stratospheric overworld air. For ^{7}Be, all of the T4 samples are below 10^{6} atoms/m^{3}, as are two of the five S4 data points. The highest ^{7}Be concentrations observed are among the T2, S2, and S3 groups ($>2 \times 10^{6}$ atoms/m^{3}), with only one S4 data point just barely above this threshold (Figure 4). Similarly, for ^{10}Be, the highest mixing ratios observed in the troposphere belong to the T2 and T3 groups (Figure 5). In the stratosphere, the highest values are S3 and S4. Note, the ^{10}Be mixing ratios should reflect mixing and removal processes alone, while the ^{7}Be mixing ratios also reflect some decay as air moves away from high production regions.

[26] T1 samples have the lowest mean mixing ratios for O_3 as well as for beryllium isotopes (Figure 6). However, unlike beryllium, O_3 mixing ratios increase with height through the stratosphere. The highest mixing ratio occurs in an S4 sample. Similarly, the next 6 highest O_3 samples are all in the S3 group. Both of these observations point to downward mixing of air from an overlying region of the stratosphere. What is unlikely to be noticed from the O_3 data alone is the stratospheric signature in samples from the T3 and T4 groups, some of which have O_3 mixing ratios very similar to most T1 data points (Figure 6). Without the beryllium ratio data, some T2 samples could be interpreted to be more heavily influenced by stratospheric air than many T3 and T4 samples. The ratio of ^{10}Be to ^{7}Be gives

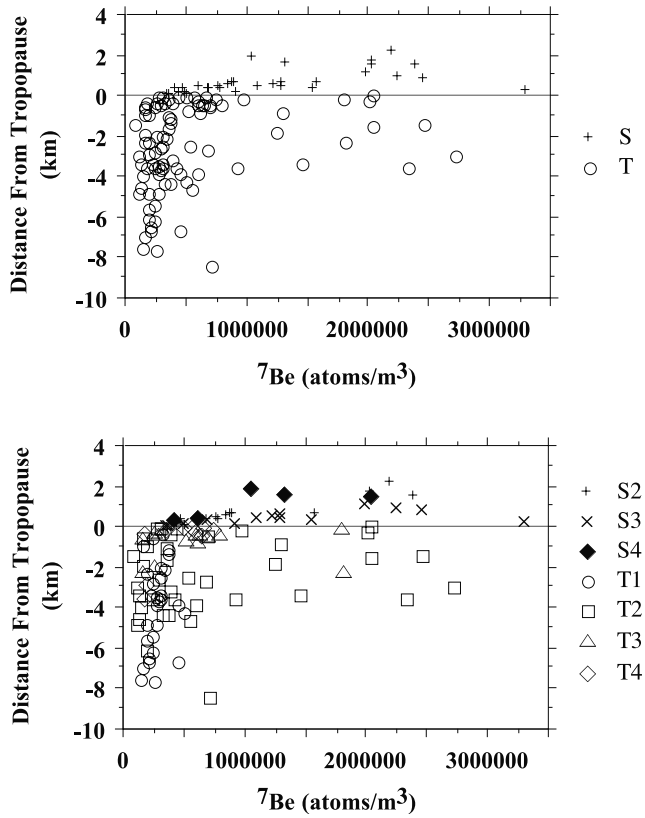

Figure 4. ^{7}Be plotted versus distance from the tropopause. Top panel shows the difference between stratospheric and tropospheric samples. Bottom panel further subdivides these according to the value of the ^{10}Be/^{7}Be ratio, the groups defined as in Figure 1 caption.

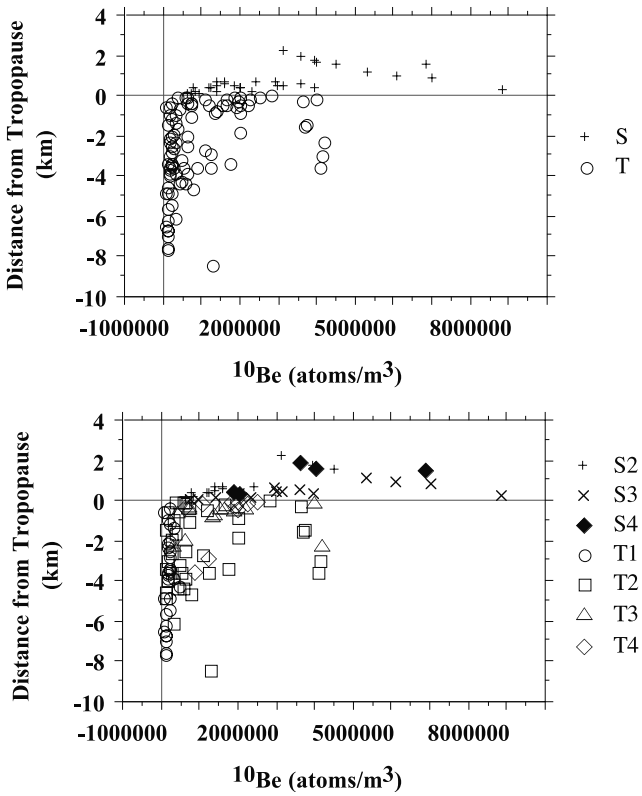

Figure 5. ^{10}Be plotted versus distance from the tropopause. Top panel shows the difference between stratospheric and tropospheric samples. Bottom panel further subdivides these according to the value of the $^{10}Be/^{7}Be$ ratio, the groups defined as in Figure 1 caption.

more information about the sources of the sampled air than the mixing ratios alone are able to reflect.

4. Discussion

[27] This data set provides information relevant to answering some of the questions about stratosphere-troposphere exchange (STE) raised in the introduction.

4.1. In Situ Production Versus Downwelling

[28] *Folkins et al.* [1999] suggested elevated O_3 between the chemopause at 14 km and the tropopause at 17 km was due to in situ production rather than mixing down from the stratosphere into the troposphere. There are 11 samples from the PEM-Tropics A mission (September and October 1996) collected between 12°S and 16°S (the *Folkins et al.* study was done at Samoa at 14°S). Unfortunately, none of the samples here was collected between 14 and 17 km, but rather were obtained between 3 and 11 km. Most of the samples (eight) were typical tropospheric samples with $^{10}Be:^{7}Be < 1.0$ and $O_3 < 100$ ppbv. The remaining three samples had ratios of 1.2, 1.4, and 3.0, with associated O_3 of 94, 74, and 112 ppbv, respectively. It is interesting that these three samples were collected between 4.5 and 7 km, with the highest ratio sample obtained at 4.5 km. These samples suggest some introduction of stratospheric air into the troposphere occurs at this latitude. There is insufficient data to resolve the question of in situ production, since none of these samples were collected between 14 and 17 km. However, it is clear that the ratio could be used to resolve this question in the future.

4.2. Tropopause Folding - PEM-West B Flight 17

[29] The Pacific Exploratory Mission - West B (PEM-West B) was part of the series of missions conducted under NASA's Global Tropospheric Experiment (GTE) program. PEM-West A and B were designed to study the effects of Asian outflow on the free troposphere over the Pacific during two different seasons (fall and spring, respectively). Flight 17 of the PEM-West B campaign was flown through a tropopause fold. This fold has been described in detail by *Dibb et al.* [1997]. The flight track included long, constant altitude legs at five levels along a SW-NE line over the Sea of Japan. The samples containing ^{7}Be and ^{10}Be during this flight are shown along with O_3, CO, CH_4, CO_2, and HNO_3 data in Table 2. The first two samples were collected at 35,000 ft (10.67 km) as the plane flew SW in and above the fold. The plane turned and headed back NE, maintaining the same altitude while two more samples were collected. The remaining samples were collected at or below 20,000 ft (6.10 km), well below the tropopause fold. The highest concentrations of both Be isotopes were observed in the first four samples. The stratospheric nature of these samples is borne out by the high O_3 (ranging from 259–479 ppbv) and HNO_3 (1031–2415 pptv) and low CO (34–51 ppbv), CH_4

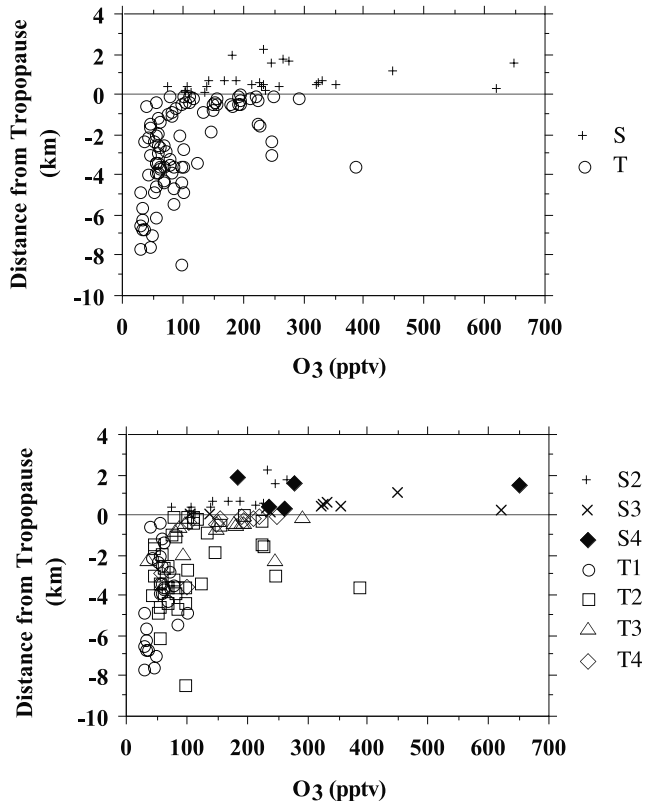

Figure 6. O_3 plotted versus distance from the tropopause. Top panel shows the difference between stratospheric and tropospheric samples. Bottom panel further subdivides these according to the value of the $^{10}Be/^{7}Be$ ratio, the groups defined as in Figure 1 caption.

Table 2. Case Studies From Three Different Flights

Sample Number	Altitude, kft	Latitude	Longitude	UT, hrs	Strat/Trop	^{7}Be, atoms/m^3 $\times 10^3$	^{10}Be, atoms/m^3 $\times 10^3$	^{10}Be/^{7}Be	O_3, ppbv	CO, ppbv	CH_4, ppbv	N_2O, ppbv	CO_2, ppmv	HNO_3, pptv
						PWB Flight 17								
						11-Mar-94								
1	35	39.232	137.717	0.87	S	1380	2780	2.01	316	41	1644	295		1031
2	35	38.825	135.348	1.40	S	930	2420	2.61	259	51	1686	301	356	1206
3	35	40.534	136.780	1.92	S	1150	3160	2.75	355	42	1637	294	355	2018
4	35	44.102	139.361	2.45	S	1740	4570	2.63	479	34	1586	284	355	2415
5	20	44.692	139.881	3.07	T	90	360	3.82	49	169	1789	311	362	270
6	20	42.088	137.804	3.52	T	20			46	144	1774	311	361	225
7	1	41.696	137.517	4.15	T		90		37	204	1836	311	365	392
8	1	43.089	138.552	4.45	T	50			36	203	1839		365	283
9	7	44.683	139.815	4.80	T	60	110	1.78	40	195	1808	311	364	120
10	11	44.388	139.605	5.25	T		100		43	211	1814	311	364	149
11	11	41.915	137.666	5.73	T	90	90	0.97	43	178	1807	311	363	155
12	11	39.701	136.201	6.20	T		90		44	167	1801	311	362	181
						SONEX Flight 8								
						25-Oct-97								
1	32	55.855	−5.130	8.82	T	340	160	0.45	42	74	1752		361	45
2	32	57.553	−2.748	9.10		280	240	0.86	56	83	1774		361	61
3	32	59.266	0.006	9.38		220	300	1.35	72	86	1765		361	233
4	37	61.708	2.613	9.78	S	800	1300	1.64	109	62	1748	312	361	305
5	37	63.268	4.774	10.08		1530	2290	1.49	166		1726		362	429
6	37	63.881	7.477	10.38	S(T)	2720	4160	1.53	245	31	1700	307	362	621
7	37	65.720	9.744	10.68	S	2200	3180	1.44	237	32	1704	307	362	692
8	37	67.921	11.815	11.00	S	2400	4550	1.90	251	32	1703	306	362	730
9	33	67.600	11.191	11.38	S	2050	3990	1.95	267	28	1690	304	362	867
10	33	65.074	9.057	11.70	S(T)	2460	3740	1.52	225	34	1705	307	362	929
11	25	65.586	9.560	12.12	T	920	1260	1.37	98	76	1759	311	362	356
12	25	67.938	11.846	12.47	T	540	630	1.18	69	89	1777	313	361	154
13	15	67.262	10.915	12.93		110	190	1.71	39	106	1819	313	362	67
14	15	65.234	9.226	13.28		130	110	0.85	40	111	1814	314	363	
15	15	63.648	6.280	13.63		170	280	1.65	52	111	1795	313	362	80
17	25	59.904	0.877	14.27		310	340	1.09	55	81	1770		361	79
18	35	57.184	−2.425	14.67	T	390	500	1.28	78	79	1760		361	155
19	35	54.812	−5.416	15.07		210	330	1.55	48	73	1749		361	85
						SONEX Flight 6								
						20-Oct-97								
1	29	50.470	−7.765	8.52		710	1880	2.66	121	52	1734	N/A	362	229
2	29	48.404	−7.431	8.83	T	190	1220	6.46	59	79	1766	N/A	361	75
3	29	44.228	−7.409	9.18		170	360	2.19	56	78	1765	N/A	361	41
4	29	43.771	−7.779	9.55		270	370	1.34	67	70	1756	N/A	361	
14	35	47.126	−6.970	13.50	T	420	530	1.24	69	65	1746	N/A	361	146
15	35	49.472	−7.021	13.78		2160	3970	1.84	260	32	1695	N/A	362	741
16	37	51.032	−6.607	13.98	S(T)	1810	4170	2.30	245	33	1702	N/A	362	782
17	37	52.451	−7.363	14.23		660	750	1.15	78	54	1740	N/A	361	350
18	33	52.458	−7.460	14.53		290	220	0.75	44	76	1761	N/A	361	110
20	27	52.333	−7.075	15.12		210	350	1.65	58	80	1767	N/A	361	82

(1586–1686 ppbv), N_2O (284–301 ppbv), and CO_2 (355–356 ppmv). The ^{10}Be:^{7}Be ratio of these samples ranges from 2.01 to 2.75 (all in the S3 category), which may indicate stratospheric air being pulled down toward the tropopause from higher altitudes as the jet weakens with the onset of spring.

[30] The remaining samples are all typical tropospheric samples (Table 2) with low O_3 (36–49 ppbv) and HNO_3 (120–392 pptv), and high CO (144–211 ppbv), CH_4 (1774–1839 ppbv), N_2O (311 ppbv), and CO_2 (361–365 ppmv). However, what these tracers do not reveal is the influence of stratospheric air on sample 5, with a ratio of 3.82 ± 0.78. This ratio puts this sample in the T4 group and suggests the presence of old stratospheric air that has descended into the lower stratosphere prior to mixing into the troposphere via the fold. While mixing and/or aerosol scavenging has removed the stratospheric signature from the observed concentrations, the ratio has preserved the presence of this component.

4.3. Mixing in the Stratosphere - SONEX Flight 8

[31] The SONEX (Subsonic Assessment, Ozone and Nitrogen Oxide Experiment) mission was conducted by NASA in October and November of 1997 to better understand the impact of aircraft exhaust on O_3, and NO_x in the free troposphere (Thompson and Singh, unpublished data, 1997, available at http://telsci.arc.nasa.gov/~sonex/pages/pg1.html). The flights were based out of Ireland, Azores, and Maine to collect samples in high air traffic regions of the North Atlantic (Thompson and Singh, unpublished data, 1997). In particular, flight 8 was a northern survey, flying from Shannon, Ireland northeast to parallel the Norwegian coast up to about 69°N. This flight path crossed the tropopause into the stratosphere (Figure 7), where a box

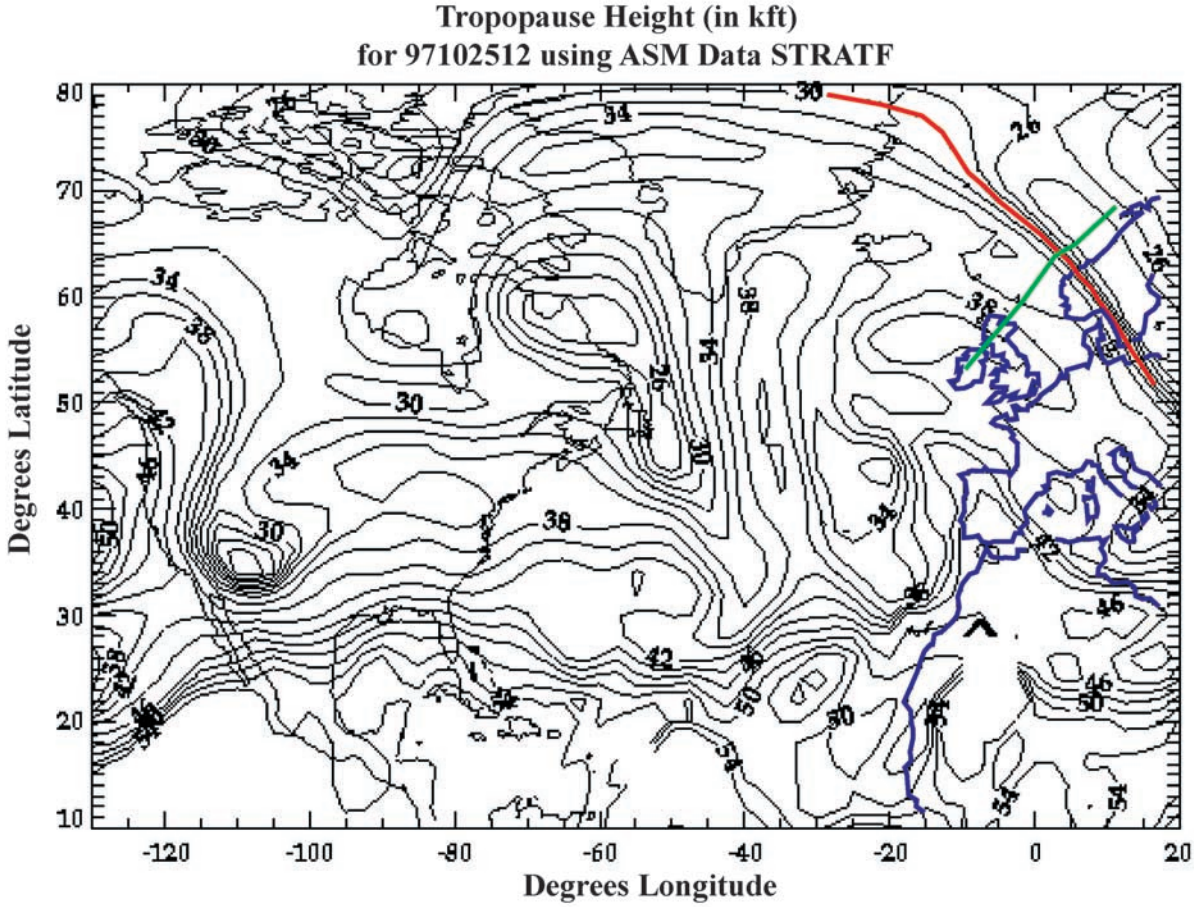

Figure 7. Contour plot of tropopause height during SONEX flight 8. 30,000 ft tropopause height contours and continental outlines near the flight path (green line) are highlighted in red and blue, respectively. [This figure courtesy of Tom Kucsera, Science Systems and Applications, Inc., Mail Code 916, NASA Goddard Space Flight Center, Greenbelt, MD 20771.]

flight plan was used to allow sampling along four constant altitude legs in the same region, with two legs in the stratosphere, one near the tropopause, and the last in the troposphere.

[32] Potential vorticity (PV) maps have been used to delineate the stratosphere (higher PV) from the troposphere (lower PV) [*Danielsen*, 1968; *Danielsen and Mohnen*, 1977; *Danielsen and Hipskind*, 1980; *Danielsen et al.*, 1987; *Browell et al.*, 1987]. These plots were produced routinely for the SONEX mission. The path of Flight 8 is superimposed onto a contour plot of the potential vorticity (Figure 8). The symmetry of the contours reflects the plane turning back on itself between samples 8 and 9, and again between samples 10 and 11 and finally between 12 and 13. The darkest orange contours are indicative of stratospheric air, while the blue end of the spectrum is tropospheric. The first three samples collected at 32,000 ft are south of the tropopause crossing point and are well within the troposphere. The chemistry of these samples reflect that; both Be isotopes, O_3, and HNO_3 have low concentrations, while CO and CH_4 are high (Table 2). Increasing HNO_3 and ^{10}Be:^{7}Be in the third sample reflects the approach to the tropopause.

[33] The next 7 samples are stratospheric, the first 5 collected at 37,000 ft and the remainder at 33,000 ft. The PV plot (Figure 8) shows the flight path crossing a gradient, which is particularly evident in the change in the chemistry of the first three samples. O_3 increases from 109 to 245 ppbv, HNO_3 increases from 305 to 621 pptv, while CO drops from 62 to 31 ppbv, and CH_4 drops from 1748 to 1700 ppbv (Table 2). The Be isotope concentrations also increase over this interval from 795×10^3 to 2716×10^3 atoms/m^3 (^{7}Be) and from 1304×10^3 to 4158×10^3 atoms/m^3 (^{10}Be). This reflects the transition zone nature of the near tropopause region both in the troposphere and the stratosphere. The ratio does not change much over this interval, nor does it over the entire set of stratospheric samples. The highest ratios, near 1.9, are observed nearest the peak in PV, samples 8 and 9 (Figure 8). Note, the sample numbers on Figure 8 are schematic, use the time in Table 2 to locate the sample along the flight leg using the *x*-axis of Figure 8. This supports the contention that the highest ratios are to be found further away from the tropopause. However, for this flight, all of the samples are S2 samples, the group that represents the youngest stratospheric samples observed. This is consistent with a suppression of downwelling of older air from the stratospheric overworld into the lower stratosphere at this time of year (late October) as discussed in the introduction.

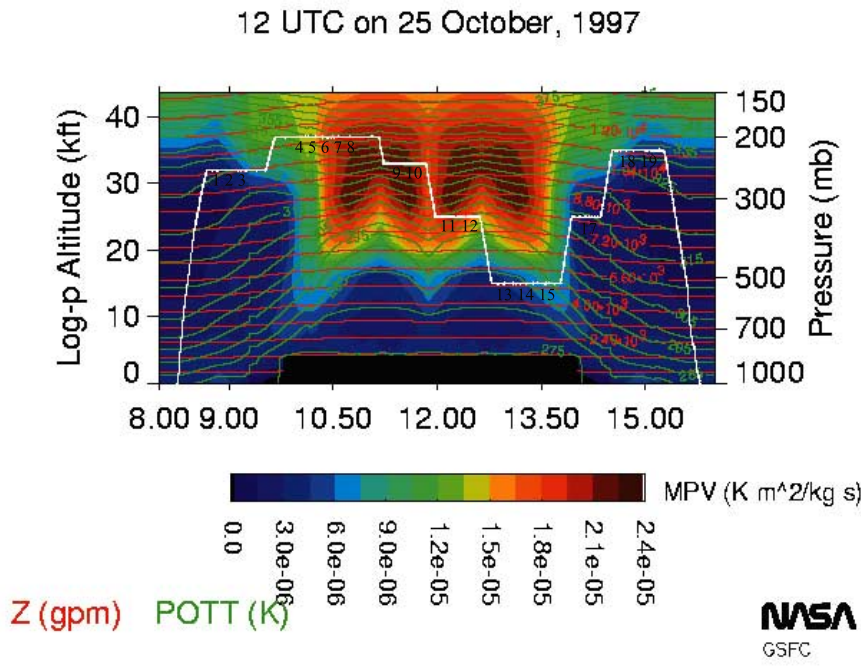

Figure 8. Potential vorticity (color contours) along SONEX flight 8 path (white). Time along the flight path is on the *x*-axis. Orange contour lines show geopotential height (m). Green contour lines show potential temperature (K). Black sample numbers indicate flight leg during which samples were collected. The symmetry of the color contours reflects the plane turning back along the same course, at four different altitudes (the 2nd through 5th level flight legs). The first two of these four altitude levels are partially or entirely within the stratosphere (dark orange colors); the last two of these are in the troposphere. [This figure courtesy of Tom Kucsera, Science Systems and Applications, Inc., Mail Code 916, NASA Goddard Space Flight Center, Greenbelt, MD 20771.]

[34] Two of the samples during this flight that were classified as tropospheric based on the MTP data clearly have stratospheric chemical characteristics (Table 2) and would be classified as that based on PV (samples 6 and 10, Figure 8). Hence the notation in the table has been modified to S(T). It has been argued that PV is a better quantity to distinguish between stratospheric air and tropospheric air [e.g., *Danielsen*, 1968; *Danielsen et al.*, 1987]. However, MTP data is available for more of the combined ^{10}Be and ^{7}Be data set than PV data and is therefore used here, even though it may sometimes yield misleading results.

4.4. Synoptic Systems - SONEX Flight 6

[35] Flight 6, also from the SONEX mission, was carried out five days earlier than flight 8 described above. This flight also originated in Shannon, Ireland, but headed south to Spain, then angled out over the Atlantic. This path cut across a particularly steep gradient in tropopause heights (Figure 9). The gradient was due to strong convection associated with a trough over the eastern Atlantic evident at both 500 hPa and 250 hPa and an associated surface cyclone located off the northwestern corner of the Iberian peninsula. Surface convergence and uplift due to the cyclone on the southern portion of the flight allowed for tropospheric air to be convected above 40,000 ft (Figures 9 and 10). A cutoff low (Figure 11) to the north of this region appears to be responsible for the sharp drop in tropopause height to below 30,000 ft just to the west of the northern portion of the flight path. The lowest tropopause height encountered by the DC-8 was at 30,000 ft on the northern part of the flight track. On the outbound leg, the altitude of the plane was 29,000 ft, approaching the tropopause, but not crossing it (Figure 9; Table 2). The four samples collected on this leg are all tropospheric, however the presence of stratospheric air is evident to varying degrees. All of the concentration data indicate the greatest stratospheric influence in the first of these four samples, both Be isotopes, O_3, and HNO_3 are highest, while CO and CH_4 are lowest for this sample. However, the beryllium ratio shows that stratospheric air has influenced all four samples, with the oldest air in the second sample, not the first. What is striking about this sample is its exceedingly high ratio of 6.46 ± 1.14. This is the highest ratio observed in the entire data set. Its presence in the troposphere suggests that old air in the stratosphere generally resides away from the tropopause where most of the stratospheric samples were collected.

[36] Another striking feature is that this is the only T4 sample collected in the fall (20 October 1997). The others were all collected during the SUCCESS mission in spring, presumably due to downwelling from the stratospheric overworld as the jet weakened. This intrusion of stratospheric air does not appear to be a tropopause fold, because the intrusion is not drawn equatorward as it descends (Figure 12) which is characteristic of folds. Another scenario for bringing stratospheric air into the troposphere involves large storm systems. This synoptic system off the coast of Spain produced rain from the northwest coast of France to the southern end of Portugal. The DC-8 reported lightning associated with con-

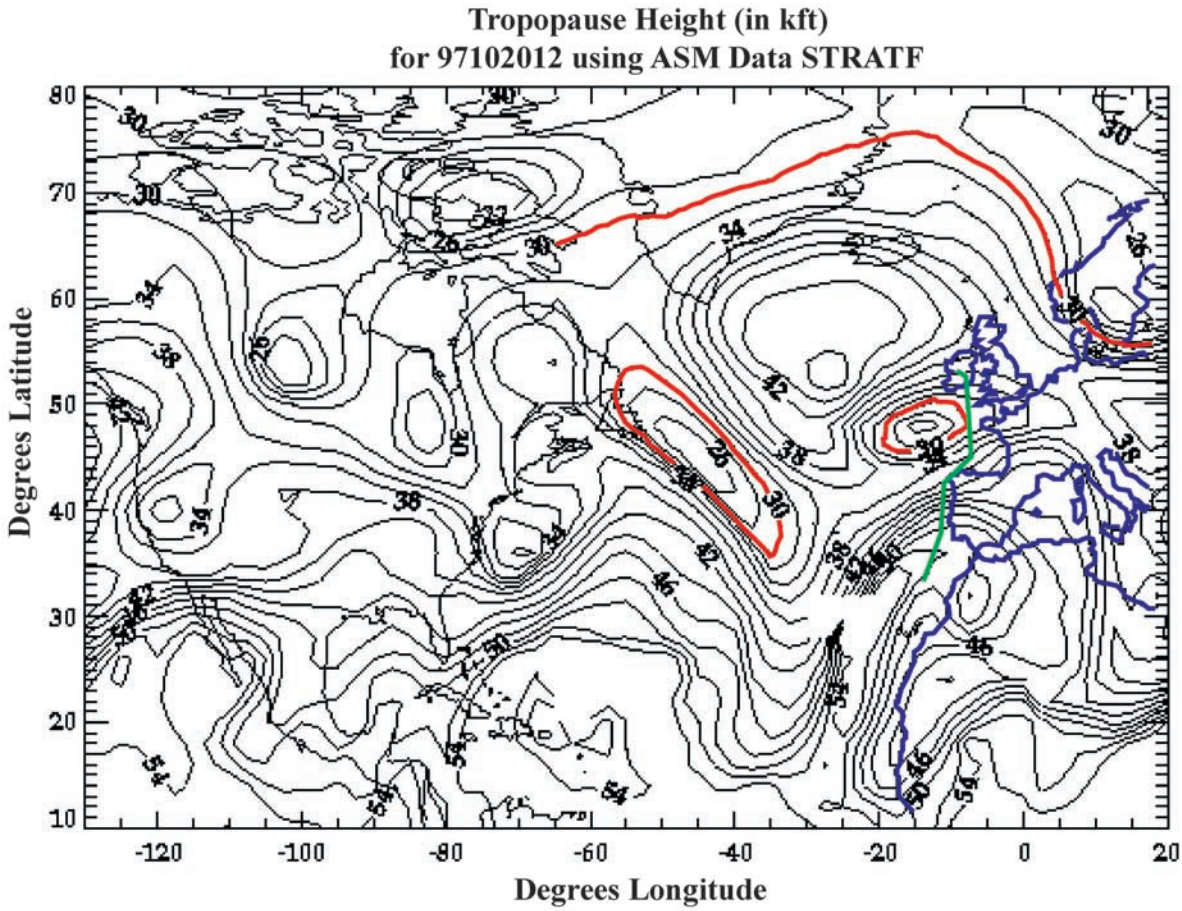

Figure 9. Contour plot of tropopause height during SONEX flight 6. 30,000 ft tropopause height contours and continental outlines near the flight path (green line) are highlighted in red and blue, respectively. [This figure courtesy of Tom Kucsera, Science Systems and Applications, Inc., Mail Code 916, NASA Goddard Space Flight Center, Greenbelt, MD 20771.]

vective cells (Thompson and Singh, unpublished data, 1997). It is likely that this cutoff low allowed the observed depression of the tropopause height, drawing stratospheric air down to low altitudes during this flight. It is not clear whether the very old stratospheric air observed descended solely because of the storm, or whether it had descended due to other processes and the storm drew it down from the lower stratosphere. Note, the concentrations of the Be isotopes are not atypical, so the high ratio is not an artifact of a particularly low amount of ^{7}Be.

[37] On the return leg, the aircraft altitude was sufficiently high to enter the stratosphere. Samples 14 and 17 appear to be very near the tropopause and reflect a blend of tropospheric and stratospheric air. Samples 15 and 16 appear to lie entirely in the lower stratosphere (Figure 10; Table 2). The last two samples are predominantly tropospheric. The ratios are consistent with this. And while one of the stratospheric samples has a ratio above 2.0 (S3), none of the other ratios reflect the presence of air as old as that observed on the outbound leg of the flight.

5. Summary

[38] We have presented the largest ^{10}Be (half-life of 1.5×10^{6} years) data set to date. Combining samples from five NASA aircraft field missions (PEM: West A and B, Tropics A; SONEX; and SUCCESS) the data set is composed of 300 samples for which the ^{10}Be:^{7}Be ratio may be determined. A subset of 123 samples for which there is also tropopause height (from temperature measurements) has been presented in detail to illustrate different properties of the ratio for stratospheric and tropospheric samples. Note that all of the stratospheric samples were obtained within 2.5 km of the tropopause; hence they represent only the lowermost stratosphere.

[39] The absence of ratios <1.27 in the lowermost stratosphere indicates that ratios observed in the troposphere, nearer the production rate of 0.60, are characteristic of tropospheric air with minimal stratospheric influence. This is corroborated by the low mixing ratios of both beryllium isotopes for such low ratio tropospheric samples. Since, aerosols do not remain in the troposphere long enough for the ratio to increase substantially after production, the presence of high ratios in the troposphere reflects stratospheric air that has entered the troposphere. In the stratosphere, only 16% of the samples had ratios above 3.0. This suggests that high ratio air tends to reside away from the tropopause.

[40] In the midlatitudes, the highest ratios are observed in the lowermost stratosphere and troposphere in the spring

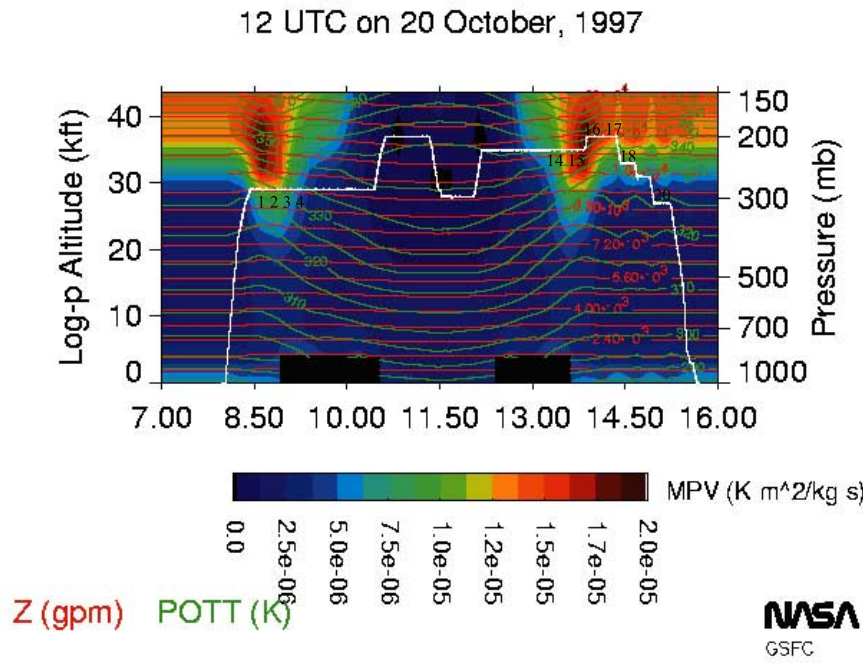

Figure 10. Potential vorticity (color contours) along SONEX flight 6 path (white). Time along the flight path is on the *x*-axis. Orange contour lines show geopotential height (m). Green contour lines show potential temperature (K). Black sample numbers indicate flight leg during which samples were collected. The blue contours show tropospheric air above 40,000 ft. While the flight path at 29,000 ft approaches the stratosphere, it does not enter it. Sample 2, collected on this flight leg, had the highest ratio observed in this data set. [This figure courtesy of Tom Kucsera, Science Systems and Applications, Inc., Mail Code 916, NASA Goddard Space Flight Center, Greenbelt, MD 20771.]

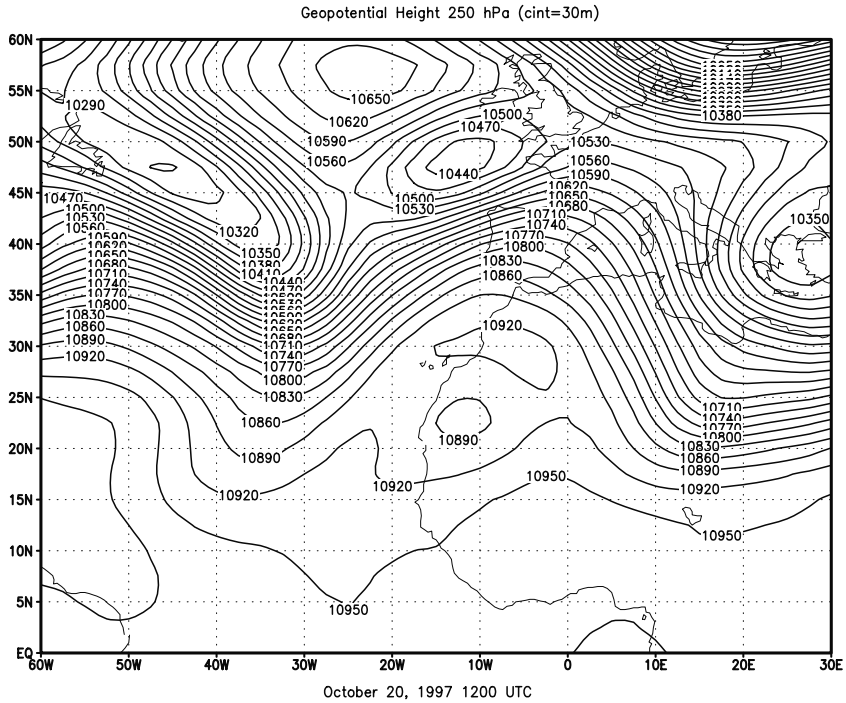

Figure 11. Geopotential height for 250 hPa shows a cutoff low to the northwest of the Iberian Peninsula. The low tropopause heights encountered on SONEX flight 6 are attributed to this low. [This figure courtesy of David Westberg, SAIC, NASA Langley Research Center, Mail Stop 483, Hampton, VA 23681, using NCEP Reanalysis data provided by the NOAA-CIRES Climate Diagnostics Center, Boulder, Colorado, USA, http://www.cdc.noaa.gov/.]

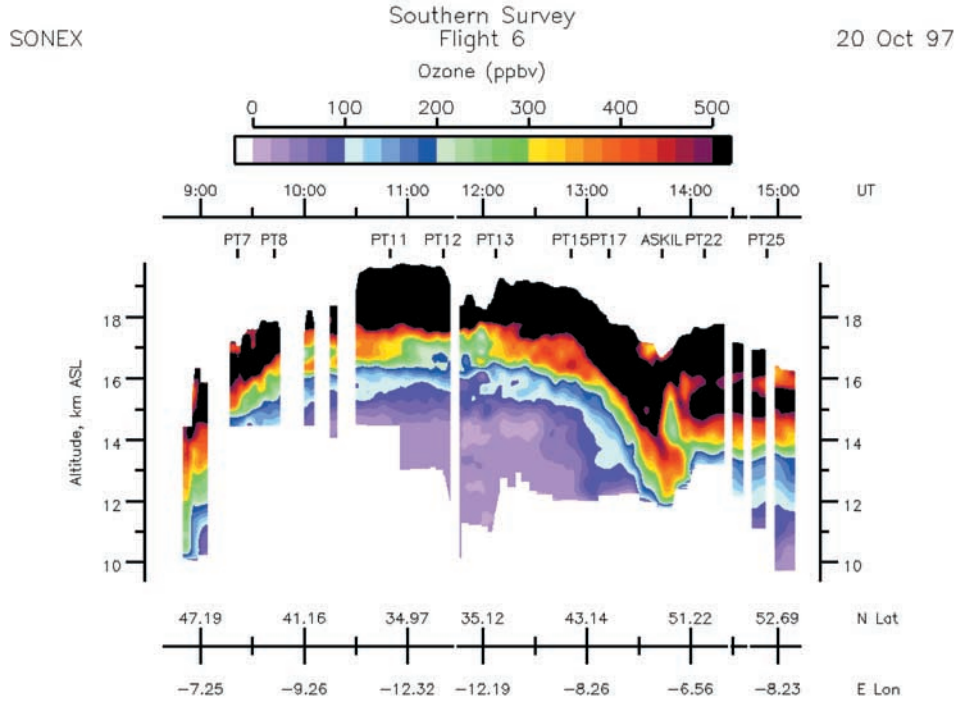

Figure 12. O_3 data from the UV DIAL instrument during SONEX flight 6. Altitude is on the *y*-axis, latitude and longitude along the flight track are on the *x*-axis. The orange and black contours indicate stratospheric air. The tongue of stratospheric air extending downward into the troposphere around 50°N is not a tropospheric fold. Folds are drawn toward the equator which is not the case here. [This figure courtesy of Edward Browell, NASA Langley Research Center, Mail Stop 483, Hampton, VA 23681.]

and summer months. This is attributed to the downwelling of high ratio air that resides at higher altitudes in the tropical stratosphere. This air descends as the subtropical jet weakens in spring and summer. At high latitudes, high ratios have also been observed in spring and summer in the lowermost stratosphere. However, in this case, the high ratios are attributed to the decay of ^{7}Be to a lower secular equilibrium value as air slowly descends in the polar vortex in winter from a region of high beryllium production to a region with lower production.

[41] The three studies described show that ^{10}Be/^{7}Be ratios, when determined in the context of other chemical constituents, can provide insight into the various mechanisms of STE including, tropopause folding, changing seasonal structure of the stratosphere and the effect of synoptic systems. From this data set, it is evident that the beryllium ratio, ^{10}Be/^{7}Be, is a sensitive tracer of stratospheric air. As such, it may be applied to various questions regarding stratospheric circulation and STE. Coupling ^{10}Be/^{7}Be data with model transport should result in a greater understanding of the processes that drive atmospheric circulation.

[42] **Acknowledgments.** The authors wish to thank John Slater for sample and target preparation, John Southon, and Marc Caffee for help with the AMS measurements, and Jan Brown for assisting with the chemical separations. Thanks also go to David Westberg, Tom Kucsera, and Edward Browell for their permission to use their figures here. The ^{10}Be analyses and interpretation were supported by NSF GEO ATM Large Scale Dynamic Meteorology Program. NASA's Subsonic Assessment and Global Tropospheric Experiment programs provided the opportunity to collect the samples and conduct ^{7}Be and ^{210}Pb analyses. Manuscript preparation was supported in part by the National Research Council. This work was performed under the auspices of the U.S. Department of Energy by the University of California, Lawrence Livermore National Laboratory under Contract No. W-7405-Eng-48.

References

Aldahan, A., G. Possnert, and I. Vintersved, Atmospheric interactions at northern high latitudes from weekly Be-isotopes in surface air, *Appl. Radiat. Isotopes*, *54*, 345–353, 2001.

Benitez-Nelson, C. R., and K. O. Buesseler, Phosphorous 32, phosphorous 37, beryllium 7, and lead 210: Atmospheric fluxes and utility in tracing stratosphere/troposphere exchange, *J. Geophys. Res.*, *104*, 11,745–11,754, 1999.

Bergmann, D. J., A. Franz, and P. Cameron-Smith, ^{7}Be and ^{10}Be tracer simulations using IMPACT, the LLNL atmospheric chemical transport model: An analysis of the sensitivity to source distributions and meteorological data, poster presented at Spring AGU Meeting, Boston, Mass., 2001.

Browell, E. V., E. F. Danielsen, S. Ismail, G. L. Gregory, and S. M. Beck, Tropopause fold structure determined from airborne lidar and in situ measurements, *J. Geophys. Res.*, *92*, 2112–2120, 1987.

Brown, L., G. J. Stensland, J. Klein, and R. Middleton, Atmospheric deposition of ^{7}Be and ^{10}Be, *Geochim. Cosmochim. Acta*, *53*, 135–142, 1989.

Danielsen, E. F., Stratospheric-tropospheric exchange based on radioactivity, ozone, and potential vorticity, *J. Atm. Sci.*, *25*, 502–518, 1968.

Danielsen, E. F., and R. S. Hipskind, Stratospheric-tropospheric exchange at polar latitudes in summer, *J. Geophys. Res.*, *85*, 393–400, 1980.

Danielsen, E. F., and V. A. Mohnen, Project Dustorm report: Ozone transport, in situ measurements, and meteorological analyses of tropopause folding, *J. Geophys. Res.*, *82*, 5867–5877, 1977.

Danielsen, E. F., R. S. Hipskind, S. E. Gaines, G. W. Sachse, G. L. Gregory, and G. F. Hill, Three-dimensional analysis of potential vorticity associated with tropopause folds and observed variations of ozone and carbon monoxide, *J. Geophys. Res.*, *92*, 2103–2111, 1987.

Davis, J. C., et al., LLNL/UC AMS facility and research program, *Nucl. Instrum. Methods Phys. Res., Sec. B*, *52*, 269–272, 1990.

Dethof, A., A. O'Neill, and J. M. Slingo, A mechanism for moistening the lower stratosphere involving the Asian summer monsoon, *Q. J. R. Meteorol. Soc.*, *125*, 1079–1106, 1999.

Dethof, A., A. O'Neill, and J. Slingo, Quantification of the isentropic mass transport across the dynamical tropopause, *J. Geophys. Res.*, *105*, 12,279–12,293, 2000.

Dibb, J. E., L. D. Meeker, R. C. Finkel, J. R. Southon, M. W. Caffee, and L. A. Barrie, Estimation of stratospheric input to the Arctic troposphere: ^{7}Be and ^{10}Be in aerosols at Alert, Canada, *J. Geophys. Res.*, *99*, 12,855–12,864, 1994.

Dibb, J. E., R. W. Talbot, K. I. Klemm, G. L. Gregory, H. B. Singh, J. D. Bradshaw, and S. T. Sandholm, Asian influence over the western North Pacific during the fall season: Inferences from lead 210, soluble ionic species and ozone, *J. Geophys. Res.*, *101*, 1779–1792, 1996.

Dibb, J. E., R. W. Talbot, B. L. Lefer, E. Scheuer, G. L. Gregory, E. V. Browell, J. D. Bradshaw, S. T. Sandholm, and H. B. Singh, Distributions of beryllium 7 and lead 210, and soluble aerosol-associated ionic species over the western Pacific: PEM West B, February–March 1994, *J. Geophys. Res.*, *102*, 28,287–28,302, 1997.

Dibb, J. E., R. W. Talbot, and M. B. Loomis, Tropospheric sulfate distribution during SUCCESS: Contributions from jet exhaust and surface sources, *Geophys. Res. Lett.*, *25*, 1375–1378, 1998.

Dibb, J. E., R. W. Talbot, E. M. Scheuer, D. R. Blake, N. J. Blake, G. L. Gregory, G. W. Sachse, and D. C. Thornton, Aerosol chemical composition and distribution during the Pacific Exploratory Mission (PEM) Tropics, *J. Geophys. Res.*, *104*, 5785–5800, 1999.

Dibb, J. E., R. W. Talbot, and E. M. Scheuer, Composition and distribution of aerosols over the North Atlantic during the Subsonic Assessment Ozone and Nitrogen Oxide Experiment (SONEX), *J. Geophys. Res.*, *105*, 3709–3717, 2000.

Folkins, I., M. Loewenstein, J. Podolske, S. J. Oltmans, and M. Proffitt, A barrier to vertical mixing at 14 km in the tropics: Evidence from ozonesondes and aircraft measurements, *J. Geophys. Res.*, *104*, 22,095–22,102, 1999.

Fujiwara, M., K. Kita, and T. Ogawa, Stratosphere-troposphere exchange of ozone associated with the equatorial Kelvin wave as observed with ozonesondes and rawinsondes, *J. Geophys. Res.*, *103*, 19,173–19,182, 1998.

Koch, D., and D. Rind, Beryllium 10/beryllium 7 as a tracer of stratospheric transport, *J. Geophys. Res.*, *103*, 3907–3917, 1998.

Kritz, M. A., S. W. Rosner, E. F. Danielsen, and H. B. Selkirk, Air mass origins and troposphere-to-stratosphere exchange associated with midlatitude cyclogenesis and tropopause folding inferred from ^{7}Be measurements, *J. Geophys. Res.*, *96*, 17,405–17,414, 1991.

Monaghan, M. C., S. Krishnaswami, and K. K. Turekian, The global-average production rate of ^{10}Be, *Earth Planet. Sci. Lett.*, *76*, 279–287, 1986.

Nagai, H., W. Tada, and T. Kobayashi, Production rates of ^{7}Be and ^{10}Be in the atmosphere, *Nucl. Instr. Methods Phys. Res. B*, *172*, 781–796, 2000.

Raisbeck, G. M., F. Yiou, M. Fruneau, J. M. Loiseaux, M. Lieuvin, and J. C. Ravel, Cosmogenic ^{10}Be/^{7}Be as a probe of atmospheric transport processes, *Geophys. Res. Lett.*, *8*, 1015–1018, 1981.

Ray, E. A., F. L. Moore, J. W. Elkins, G. S. Dutton, D. W. Fahey, H. Vomel, S. J. Oltmans, and K. H. Rosenlof, Transport into the Northern Hemisphere lowermost stratosphere revealed by in situ tracer measurements, *J. Geophys. Res.*, *104*, 26,565–26,580, 1999.

Schoeberl, M. R., L. R. Lait, P. A. Newman, and J. E. Rosenfield, The structure of the polar vortex, *J. Geophys. Res.*, *97*, 7859–7882, 1992.

Shapiro, M. A., and J. L. Forbes-Resha, Mean residence time of ^{7}Be-bearing aerosols in the troposphere, *J. Geophys. Res.*, *81*, 2647–2649, 1976.

Tuck, A. F., et al., The Brewer Dobson circulation in the light of high altitude in situ aircraft observations, *Q. J. R. Meteorol. Soc*, 1997.

J. E. Dibb, Climate Change Research Center, University of New Hampshire, Durham, NH 03824, USA. (Jack.Dibb@unh.edu)

R. C. Finkel, Center for Accelerator Mass Spectrometry, Lawrence Livermore National Laboratory, MS L-202, Livermore, CA 94550, USA. (Finkel1@llnl.gov)

C. E. Jordan, National Research Council, NASA Langley Research Center Building 1250, MS 483, Hampton, VA 23681, USA. (c.e.jordan@larc.nasa.gov)